A Holographic Approach to Dense Matter in Neutron Stars

Christian Ecker

GOETHE UNIVERSITÄT FRANKFURT AM MAIN

AstroCoffee – 14 July 2020

partly based on 1908.03213 (PRD)

with Matti Järvinen, Govert Nijs and Wilke van der Schee

Outline

1. Introduction

Motivation

- Since GW170817 we detect gravitational waves (GW) and their electromagnetic counterpart from neutron star (NS) mergers.
- This enables us to collect information about dense matter inside the stars and hopefully learn something about quantum chormodynamics (QCD).
- An important tool to interpret observations are numerical simulations.
- Microphysical input needed: Equation of State (EoS), viscosities, resistivity, ...
- In practice it is prohibitively hard to compute this directly from QCD at intermediate densities and low temperatures.
- Strategy:
  - i Mimic QCD with holographic model, parameters fixed with lattice data and perturbative QCD where they are valid
  - ii Compute EoS, etc. with the tuned model at densities where traditional QCD methods fail.
  - iii Use EoS in merger simulations to produce predictions (PSD, formation of quark matter?, ...).

QCD Phase Diagram and EoS

EoS $p(\epsilon, T, \ldots)$ required to close equations of motion in an effective fluid description of neutron stars, but unfortunately it is not known because:

- Lattice QCD works only at zero/small chemical potentials
- Perturbative QCD works only at asymptotically high densities
- Effective nuclear matter models work at small densities

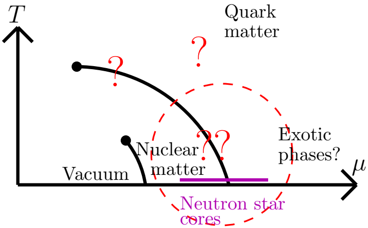

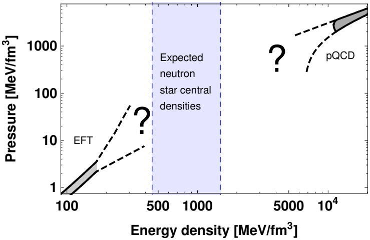

Constraints on the EoS

From theory:

- By causality the speed of sound has to satisfy: $c_s^2 = \left(\frac{\partial p}{\partial \epsilon}\right)_s < 1$.
- QCD is asymptotically free at large densities: $c_s^2 \to 1/3$.

From observation:

- NS-white dwarf binaries PSR J0348+0432: $M_{\mathrm{max}} > 2.01 \pm 0.04 M_\odot$.

  [Cromartie et al. arXiv:1904.06759, Antoniadis et al. arXiv:1304.6875]

  recently deduced from GW190814: $M_{\mathrm{max}} > 2.08 \pm 0.04 M_\odot$

  [Most, Papenfort, Weih, Rezzolla, arXiv:2006.14601]

- GW170817 constrains tidal deformability: $\Lambda \lessapprox 580$.

  [LIGO/Virgo: arXiv:1710.05832, arXiv:1805.11579, arXiv:1805.11581]

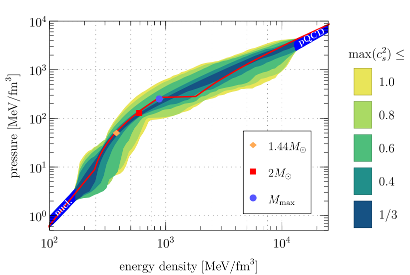

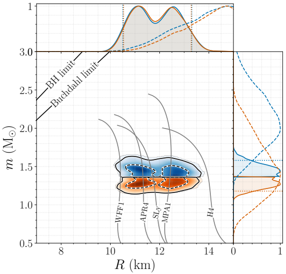

[Annala, Gorda, Kurkela, Nättila, Vuorinen arXiv:1903.09121, left plot by T. Gorda]

2. AdS/CFT Correspondence

The Holographic Principle

Any theory of quantum gravity has an equivalent description in terms of lower dimensional theory without gravity.

[t' Hooft arXiv:9310006, Susskind arXiv:940989]

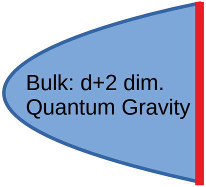

Inspired by the Bekenstein-Hawking formula (area law) for black hole entropy

$$S_{\mathrm{BH}} = \frac{c^3}{4G_{\mathrm{N}}\hbar}A \tag{1}$$

A precise realization of the holographic principle, called the AdS/CFT correspondence, was found in 1997 by Juan Maldacena in string theory.

AdS/CFT Correspondence

Type IIB string theory on $AdS_5 \times S_5$ $=$ SU(N) $\mathcal{N} = 4$ Super Yang-Mills (SYM) theory on $\mathcal{M}_4$

[Maldacena arXiv:9711200]

- The correspondence is conjectured to hold for any value of the 't Hooft coupling $\lambda = 2g_{YM}^2 N$ and rank of gauge group N.
- AdS/CFT is a strong-weak duality: if field theory is strongly coupled the gravity theory is weakly coupled and vice versa.
- **Supergravity limit:** Assuming point like strings ($\ell_s \to 0$) and small coupling ($g_s \ll 1$) reduces the string theory side to classical supergravity.
- This corresponds to the $N \to \infty$ and $\lambda \to \infty$ limit on the field theory side
- AdS/CFT as a Tool: Observables in strongly coupled field theory (very hard) can be obtained from classical gravity calculations (much easier).

The Gravity Side: AdS Spacetime

- AdS_{d+1} is a maximally symmetric solution of the Einstein equations with negative cosmological constant Λ and negative curvature radius L.

$$R_{\mu\nu} - \frac{1}{2} R g_{\mu\nu} + \Lambda g_{\mu\nu} = 0\,, \quad \Lambda = -\frac{d(d-1)}{2L^2}$$

- This is different from our universe which is well described by de Sitter space with small positive cosmological constant $\Lambda = 1.1056 \times 10^{-52}\,\mathrm{m}^{-2}$.
- AdS space has a timelike boundary at $r = \infty$, which for the Poincaré patch is Minkowski space. In the AdS/CFT context this is where the CFT lives.

$$ds^2 = \frac{L^2}{r^2} dr^2 + \frac{r^2}{L^2} \underbrace{\left(-dt^2 + d\vec{x}^2\right)}_{\text{boundary metric}}$$

- Asymptotic AdS spacetimes, like the AdS black brane, look only at $r \to \infty$ like AdS, but differ in the interior, e.g. by the presence of a BH horizon.

The Holographic Dictionary

- Every quantity on the gravity side corresponds to a dual quantity on the field theory side.

Gravity Side	Gauge Theory Side
black hole area $\mathcal{A}$	thermal entropy $S_{\rm th}$
on-shell action $S_{\rm grav}$	f free energy
metric $g_{\mu\nu}$	$T^{\mu\nu}$ stress tensor
scalar field ϕ	$\mathcal{O}$ scalar operator
gauge field A_μ	J^μ global sym. current
...	...

- Geometry in the bulk corresponds to a state in the field theory:
  e.g.: black hole geometries correspond to finite temperature states with T equal the Hawking temperature of the BH.
- Sometimes there are multiple gravity solutions, which correspond to different phases in the field theory.
  The thermodynamicaly preferred (stable) phase is the one with lowest free energy, i.e., smaller $S_{\rm grav}$.

3. Holographic QCD

Holographic QCD

The total gravity action ($S_{\rm grav}$) consists of a gluon (S_g) and a flavour (S_f) part:

$$S_{\rm grav} = S_g + S_f \tag{2}$$

Gluon part (Einstein-dilaton gravity):

$$S_g = N_c^2 M_{\rm Pl}^3 \int d^5x \sqrt{-g} \left(R - \frac{1}{2} \partial_\rho \phi \, \partial^\rho \phi - V(\phi) \right) \tag{3}$$

Dilaton $e^\phi \leftrightarrow \mathrm{Tr} F^2$ sources the 't Hooft $\lambda = g_{\rm YM}^2 N_c$ coupling in YM theory.

Flavour part (tachyonic Dirac-Born-Infeld action):

$$S_f = -N_f N_c M_{\rm Pl}^3 \int d^5x \mathcal{Z}(\phi,\chi) \sqrt{-\det\left(g_{\mu\nu} + \kappa(\phi,\chi)\partial_\mu\chi\partial_\nu\chi + \mathcal{W}(\phi,\chi)F_{\mu\nu}\right)} \tag{4}$$

Tachyon $\chi \leftrightarrow \bar{q}q$ controls chiral symmetry breaking, Abelian field strength $F_{\mu\nu} = \partial_\mu A_\nu - \partial_\nu A_\mu$ determines dynamics for the U(1) gauge field A_μ, boundary value of A_0 gives quark-chemical potential μ in the field theory.

Several potentials $\{V, \mathcal{Z}, \kappa, \mathcal{W}\}$ either fixed by string theory construction (top-down) or matched to pQCD and lattice QCD (bottom-up).

[For details and references see e.g. Hoyos et al. arXiv:2005.14205; Ishii et al. arXiv:1903.06169]

$\mathcal{N} = 4$ SYM + probe matter

Top-down: e.g. D3-D7 model, potentials entirely fixed by string construction

$$M_{\rm Pl}^3 = \frac{1}{8\pi^2},\ \mathcal{Z} = \frac{\lambda_{\rm YM}}{2\pi^2}\cos^3\chi,\ \mathcal{W} = \frac{2\pi}{\sqrt{\lambda_{\rm YM}}},\ \kappa = 1,\ \lambda_{\rm YM} \simeq 10.74 \qquad (5)$$

[Karch, O' Bannon, arXiv:0709.0570]

Combine D3-D7 model ($\epsilon = 3p + \frac{3m^2}{2\pi}\sqrt{p}$) with soft, intermediate and stiff nuclear matter EoS.

[Hebeler, Lattimer, Pethick, Schwenk arXiv:1303.4662]

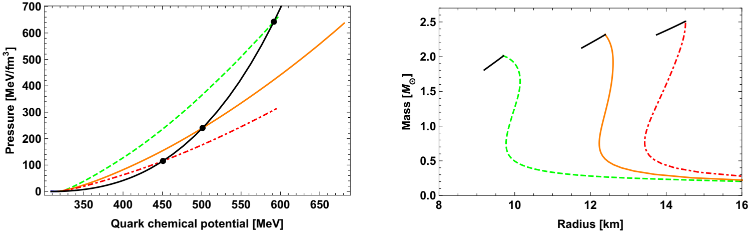

[Hoyos, Fernandez, Jokela, Vuorinen arXiv:1603.02943]

- Strong first order nuclear to quark matter phase transition.
- Neutron stars with holographic quark matter cores are unstable.
- Varying the quark mass m on can also get stable quark and hybrid stars.

[Annala, CE, Hoyos, Jokela, Fernandez, Vuorinen arXiv:1711.06244]

Veneziano QCD

Bottom-up: $S_g + S_f$ in Veneziano limit (=V-QCD), maintains backreaction between quarks and gluons

$$N_c \to \infty \text{ and } N_f \to \infty \text{ with } x \equiv N_f/N_c \text{ fixed}$$

[Järvinen, Kiritsis arXiv:1112.1261]

Form of the potentials $\{V, \mathcal{Z}, \kappa, \mathcal{W}\}$ guided by string theory, parameters fitted to lattice data near $\mu = 0$ and tuned to pQCD for small λ.

[Jokela, Järvinen, Remes, arXiv:1809.07770]

Recently: baryons in simple probe approximation as homogeneous bulk soliton

[Ishii, Järvinen, Nijs arXiv:1903.06169]

- One free parameter: b = coupling between baryon and chiral condensate.
- Non-trivial nuclear and quark matter EoS from the same model.

Phase Diagram

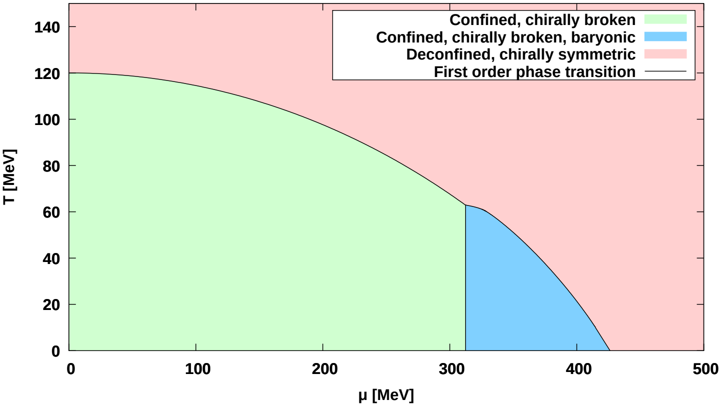

[Ishii, Järvinen, Nijs, JHEP 1907 (2019) 003]

Equation of State

- Homogeneous baryon ansatz only a good approximation at high densities: match low density region to SLy nuclear matter EoS.
  [Douchin, Haensel, Astron.Astrophys. 380 (2001) 151]
- Strong[1] first order nuclear to quark matter phase transition.
- LIGO observation GW170817 constrains $b \gtrapprox 10.45 \rightarrow \Lambda_{1.4} \approx 680$.
  [Abbott et al., Phys.Rev.Lett. 121 (2018) no.16, 161101]

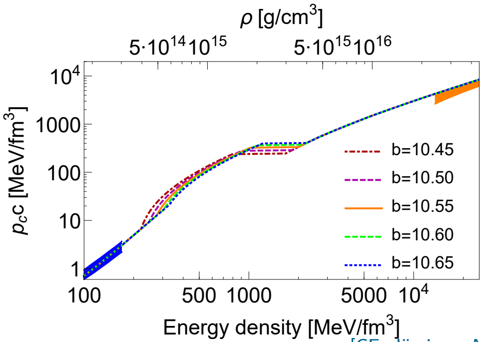

b	$\frac{\rho_m}{\rho_s}$	$\Lambda_{1.4}$
10.45	1.44	680
10.50	1.61	550
10.55	1.77	470
10.60	1.94	410
10.65	2.10	370
SLy	–	300

[CE, Järvinen, Nijs, van der Schee, arXiv:1908.03213]

[1] The latent heat at the transition is sizable (for $b = 10.5$: $\Delta\epsilon = 920\mathrm{MeV/fm}^3$).

Mass-radius relation

- Large values of $b \gtrsim 10.65$ are ruled out by $2.01 M_\odot$-bound from PSR J0348+0432 and PSR J1614-2230.

  [Antoniadis et. al., Science 340 (2013) 6131]

- Allowed values in the holographic model: $10.45 \lesssim b \lesssim 10.65$.

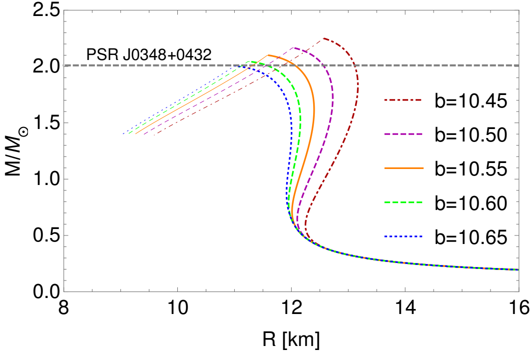

b	$\frac{R_{1.4}}{km}$	$\frac{M_{\max}}{M_\odot}$
10.45	13.0	2.25
10.50	12.6	2.17
10.55	12.3	2.10
10.60	12.1	2.04
10.65	12.0	2.00
SLy	11.7	2.05

[CE, Järvinen, Nijs, van der Schee, arXiv:1908.03213]

Mass-radius relation

- Large values of $b \gtrapprox 10.6$ are ruled out by $2.08 M_\odot$-bound deduced from GW190814.

[Most, Papenfort, Weih, Rezzolla, arXiv:2006.14601]

- Allowed values in the holographic model: $10.45 \lessapprox b \lessapprox 10.60$.

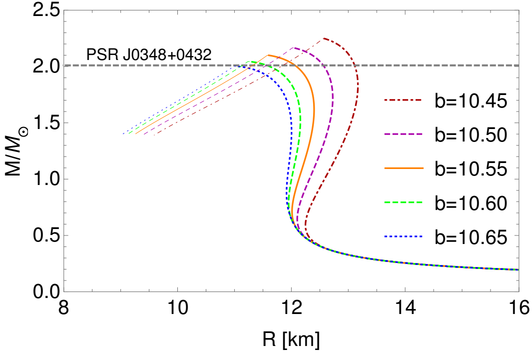

b	$\frac{R_{1.4}}{km}$	$\frac{M_{\rm max}}{M_\odot}$
10.45	13.0	2.25
10.50	12.6	2.17
10.55	12.3	2.10
10.60	12.1	2.04
10.65	12.0	2.00
SLy	11.7	2.05

[CE, Järvinen, Nijs, van der Schee, arXiv:1908.03213]

Constraining the EoS with holography

All viable hybrid EoSs (light red) compared to interpolated EoSs (light blue), both passing constraints on $M_{\max}$ and Λ.

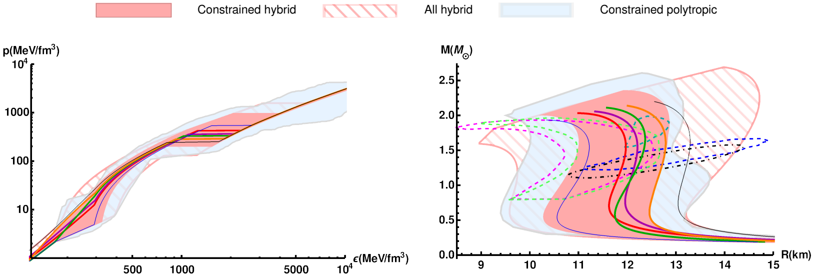

[Jokela, Järvinen, Nijs, Remes arXiv:2006.01141]

- Results disfavor stiff models at low density and soft models at high density.
- Generically strong first order nuclear to quark matter phase transition: $\Delta\epsilon \gtrapprox 500 MeV/fm^3$.
- Large radii of neutron stars preferred.

3. Merger Simulations

Merger simulations (poor man's version)

We evolve ideal general relativistic hydrodynamic equations using:

- `LORENE+EinsteinToolkit+WhiskyTHC`
- Equal mass binaries initially 45 km apart: 3-6 orbits before merger.
- Reflection symmetry across $z = 0$, but no 180°-symmetry.
- `Carpet` with 6 refinement levels and finest resolution of $368m$.
- Conformal and Covariant Z4 (CCZ4) formulation
- Cold holographic EoS with thermal component $\Gamma_{th} = 1.75$.
- Pilot project for 500k core-hours on Dutch supercomputer (Cartesius). Typical run: 2-3 days with 100 cores for $\approx 50ms$.

Neutron star merger with holographic EoS

Merger Dynamics and Waveforms

- $M = 1.3 + 1.3 M_\odot$: Formation of a long lived ($> 40ms$) HMNS.

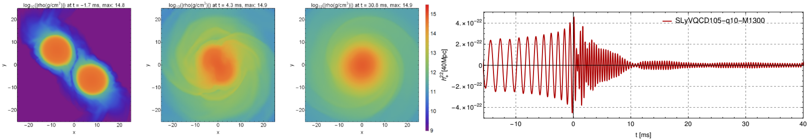

- $M = 1.4 + 1.4 M_\odot$: Formation of a short lived ($\approx 7.8ms$) HMNS.

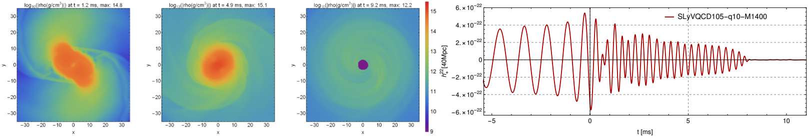

- $M = 1.5 + 1.5 M_\odot$: Prompt collapse to BH with dilute matter torus.

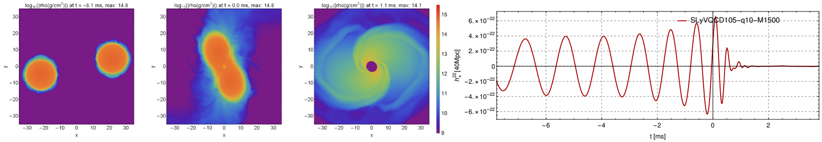

Intermediate Mass Binary

- Softening of EoS in the quark matter phase leads to phase transition induced collapse.

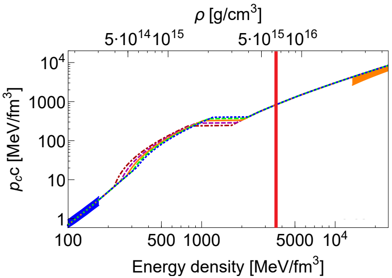

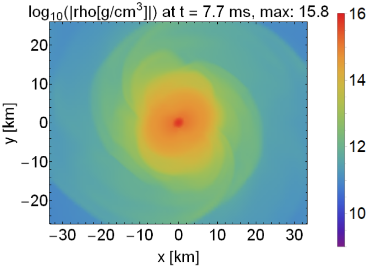

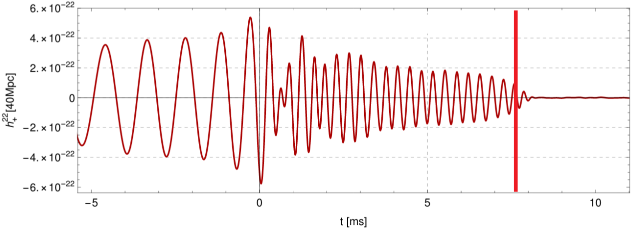

Power Spectral Density

Post-merger power spectral density (PSD) has typical three peak structure.

$$\tilde{h}(f) \equiv \sqrt{\frac{|\tilde{h}_+(f)|^2+|\tilde{h}_\times(f)|^2}{2}}\,, \quad \tilde{h}_{+,\times}(f) \equiv \int h_{+,\times}(t)e^{-i2\pi ft}dt\,.$$

Characteristic frequencies f_1, f_2, f_3 contain information about EoS.

[Takami, Rezzolla, Baiotti arXiv:1403.5672]

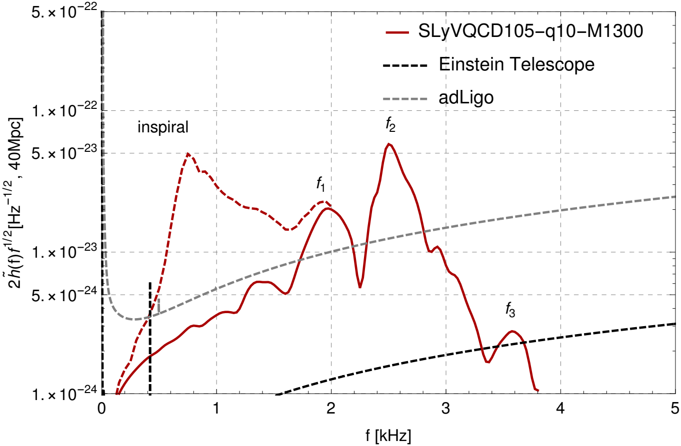

Mass dependence of the Power Spectral Density

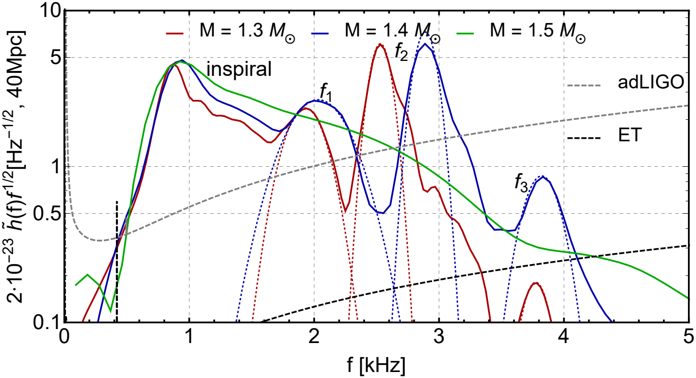

$M[M_\odot]$	EoS	b	f_1[kHz]	f_2[kHz]	f_3[kHz]
1.30	SLyVQCD105	10.5	1.93	2.53	3.77
1.35	SLyVQCD105	10.5	1.95	2.60	3.53 (3.90)
1.40	SLyVQCD105	10.5	2.03	2.89	3.82
1.50	SLyVQCD105	10.5	–	–	–

EoS dependence of the Power Spectral Density

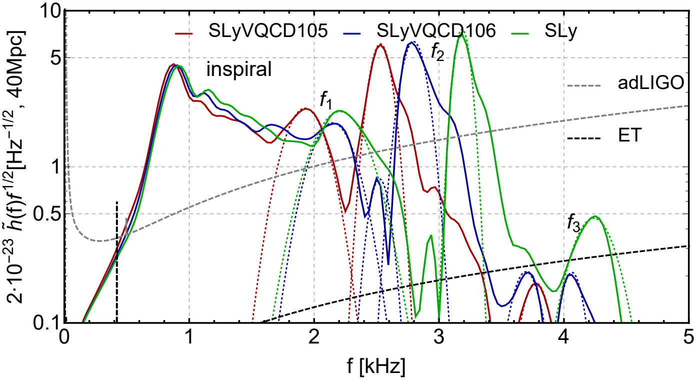

$M[M_\odot]$	EoS	b	f_1[kHz]	f_2[kHz]	f_3[kHz]
1.30	SLyVQCD105	10.5	1.93	2.53	3.77
1.30	SLyVQCD106	10.6	2.15	2.80	3.70 (4.06)
1.30	SLy	-	2.21	3.19	4.24

Universality

- Frequency f_1 as function of compactness $\mathcal{C} = M/R$ shows universal behaviour, i.e. results for different EoS fall on one universal curve.
- V-QCD EoS for $b = 10.5$ gives f_1 close to universal curve, $b = 10.6$ slightly off (?) $\implies$ more analysis needed.

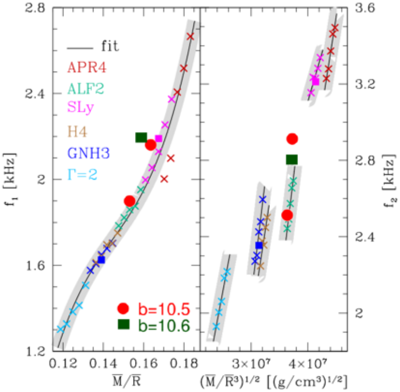

[plot from Takami, Rezzolla, Baiotti arXiv:1403.5672]

Finite Temperature EoS from V-QCD

EoS of quark matter V-QCD model combined with DD2, IUF and SFx nuclear matter EoS.

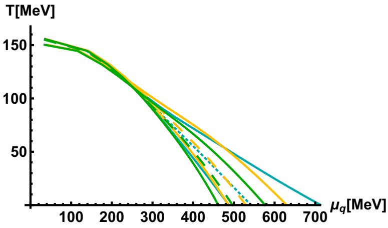

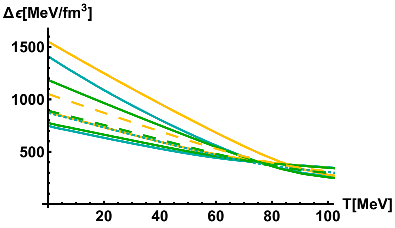

[Chesler, Loeb, Jokela, Vuorinen, arXiv:1906.08440]

- Reasonable EoS for all values of μ an T.
- Sizable latent heat at the phase transition, decreases with T.

4. Summary

Summary

- Holographic QCD provides a framework to compute microphysical parameters at finite density and T.
- V-QCD has non-trivial nuclear and quark matter EoS with first order phase transition in the same model.
- Provides a strong coupling alternative to traditional approaches.
- First application in NS merger simulations gives reasonable results.
- Preliminary lesson: strong coupling approach disfavours stable quark matter cores and leads to phase transition induced collapse in neutron star mergers.

Backup

V-QCD without baryons (I)

Consider first the non-baryonic V-QCD action, whose solutions will serve as background for the probe baryons

$$S^{(0)}_{\mathrm{V-QCD}} = S_{\mathrm{glue}} + S^{(0)}_{\mathrm{DBI}} \,.$$

The gluon part is given by the IHQCD (dilaton gravity) action

$$S_{\mathrm{glue}} = N_c^2 M^3 \int d^5x \sqrt{-g} \left[R - \frac{4}{3}\frac{(\partial\lambda)^2}{\lambda^2} + V_g(\lambda) \right],$$

where $\lambda \equiv e^{\phi} \leftrightarrow \mathrm{Tr} F^2$ ($\approx g^2 N_c$ near the boundary) sources the 't Hooft coupling in YM theory, the dilaton potential is chosen[2] to mimic QCD

$$V_g(\lambda) = 12 \left[1 + V_1 \lambda + \frac{V_2 \lambda^2}{1+\lambda/\lambda_0} + V_{\mathrm{IR}} e^{-\lambda_0/\lambda} (\lambda/\lambda_0)^{4/3} \sqrt{\log(1+\lambda/\lambda_0)} \right] .$$

Finite T is implemented by homogeneous+isotropic black brane metric

$$ds^2 = e^{2A(r)} (-f(r) dt^2 + d\vec{x}^2 + f^{-1}(r) dr^2) \,.$$

[2] E.g. V_1 and V_2 are fixed by requiring the UV RG flow of the 't Hooft coupling to be the same as in QCD up to two-loop order.

V-QCD without baryons (II)

The flavor part is modelled by the tachyonic DBI-action[3]

$$S_{\rm DBI}^{(0)} = -N_f N_c M^3 \int d^5x\, V_{f0}(\lambda) e^{-\tau^2} \sqrt{-\det\left[g_{ab} + \kappa(\lambda)\partial_a\tau\partial_b\tau + w(\lambda)F_{ab}\right]}\,,$$

$$F_{rt} = \Phi'(r)\,, \quad \Phi(0) = \mu\,,$$

where the tachyon $\tau \leftrightarrow \bar{q}q$ controls chiral symmetry breaking.

Several potentials: $\{V_g(\lambda), V_{f0}(\lambda), w(\lambda), \kappa(\lambda)\}$, chosen to match pQCD in UV ($\lambda \to 0$), qualitative agreement with QCD in IR ($\lambda \to \infty$) and tuned to lattice QCD in the middle ($\lambda \sim \mathcal{O}(1)$).

[For details see Appendix B of Ishii, Järvinen, Nijs arXiv:1903.06169]

Different solutions:

without/with horizon ↔ confined/deconfined phase
without/with tachyon ↔ chirally symmetric/chirally broken phase

---

[3]Without baryons we have a vectorial flavor singlet gauge field $A^{(L/R)} = \mathbb{I}_f \Phi(r) dt$ giving nonzero charge density and chemical potential.

Probe baryons in V-QCD

Each baryon maps to a solitonic "instanton" configuration of non-Abelian gauge fields in the bulk.

[Witten; Gross, Ooguri; . . .]

Consider the full non-Abelian brane action $S = S_{\rm DBI} + S_{\rm CS}$ where

[Bigazzi, Casero, Cotrone, Kiritsis, Paredes; Casero, Kiritsis, Paredes]

$$S_{\rm DBI} = -\frac{1}{2} M^3 N_c \, \mathbb{T}r \int d^5x \, V_{f0}(\lambda) e^{-\tau^2} \left(\sqrt{-\det \mathbf{A}^{(L)}} + \sqrt{-\det \mathbf{A}^{(R)}} \right) ,$$

$$\mathbf{A}^{(L/R)}_{MN} = g_{MN} + \delta^r_M \delta^r_N \kappa(\lambda) \tau'(r)^2 + \delta^{rt}_{MN} w(\lambda) \Phi'(r) + w(\lambda) F^{(L/R)}_{MN}$$

gives the dynamics of the solitons.
The Cern-Simons term sources the baryon number for the solitions

$$S_{\rm CS} = \frac{N_c}{8\pi^2} \int \Phi(r) e^{-b\tau^2} dt \wedge \left(F^{(L)} \wedge F^{(L)} - F^{(R)} \wedge F^{(R)} + \cdots \right) .$$

Non-Abelian DBI action only known to first few orders in $F^{(L/R)}$: expand to second order on top of solution $(g_{MN}, \Phi, \lambda, \tau)$ obtained from $S^{(0)}_{V-QCD}$.

Homogeneous Baryon Ansatz

Set $N_f = 2$ and consider the SU(2) Ansatz

[Rozali, Shieh, Van Raamsdonk, Wu]

$$A_L^i = -A_R^i = h(r)\sigma^i$$

Immediate consequence: baryon charge integrates to zero?

$$N_b \propto \int dr \frac{d}{dr}\left[e^{-b\tau^2} h^3(1 - 2b\tau^2)\right] \stackrel{?}{=} 0$$

However finite baryon number may can be realized by discontinuity of h $\leftrightarrow$ smeared solitons in singular gauge.

[Ishii, Järvinen, Nijs, arXiv:1903.06169]

The free parameter b of the model is used to tune the baryon onset to its physical value in QCD.